





and 3000 rpm for 10 s and 30 s, respectively. The substrate was then baked at 350 °C for 10 min to remove organic residuals. These spin-coating steps were repeated for 6 times to keep the thin film thickness of roughly 250 nm. These thin films were finally annealed in an environment of Ar and H<sub>2</sub> at 500 °C for 1 h. The structural properties of thin films were investigated by X-ray diffraction (XRD) (PANalytical, 18 kW rotating anode X-ray generator, Japan) with Cu-K $\alpha$  radiation ( $\lambda = 0.154056$  nm) in  $\theta$ -2 $\theta$  scan mode and field emission scanning electron microscopy (FE-SEM, 3.0 kV) (JEOL JSM-6700F, Japan). Surface roughness of thin films was observed by an atomic force microscope (AFM) (Veeco D3100) with a Nanoscope IV controller operated at tapping mode. The electrical properties were measured by four point probe (Napson, RT-70/RG-5, Japan) and Hall-effect measurement (Ecopia, HMS-3000) using the Van der Pauw method. The optical properties were measured by a UV-VIS spectrometer (JASCO, V-570, Japan).

### 3. Results and discussion

Fig. 2 shows plan-view SEM images of AZO:rGO thin films on glass substrates as a function of the rGO ratio. All of the films appeared to have been coated with rGO flakes, which had diameters ranging from 30 to 150 nm. The diameters of the rGO flakes increased with the rGO ratio, and their shape changed from small irregular shapes to large hexagon-like shapes. Fig. 3 shows cross section SEM images of AZO:rGO thin films with different rGO ratios. The average thickness of the thin films was  $250 \pm 10$  nm.

To explore the composition of the composite films, energy dispersive X-ray spectroscopy analysis of AZO:rGO thin films with different rGO ratios was performed. Table 1 lists the element ratios in AZO:rGO films with rGO ratios of 0.0 wt% and 1.0 wt%. The amounts of C and O on the film surface increased with the amount of rGO. This result is consistent with the findings in Fig. 2. The reduced Zn content in the 1.0 wt%-rGO film is attributable to rGO flakes covering the film surface. The detected Al concentration does not obviously change and is around 7–8 at%.

**Table 1**  
Element analysis of the AZO:rGO films from the EDS analysis.

Element	Weight%		Atomic%	
	0.0 wt%	1.0 wt%	0.0 wt%	1.0 wt%
C	6.28	10.59	13.84	19.56
O	35.21	46.58	38.08	48.64
Al	7.39	11.58	7.39	7.89
Zn	51.12	31.25	40.69	23.91
Totals	100.00	100.00	100.00	100.00

Fig. 4 shows atomic force microscopy images of AZO:rGO thin films with different rGO ratios. The roughness values of the thin films were 2.05, 10.08, 13.81, and 42 nm for rGO ratios of 0, 1.0, 1.5, and 3.0 wt%, respectively. The surface roughness increased with the rGO content because the size of the rGO flakes increased with the rGO content, as shown in the scanning electron microscopy images.

Fig. 5 shows XRD patterns of AZO:rGO thin films with different rGO ratios. All films showed a (0 0 2) peak at  $2\theta \approx 34^\circ$ , indicating that the AZO:rGO thin films prepared using the sol-gel method had a hexagonal wurtzite structure and favorable *c*-axis orientation perpendicular to the substrate. The (0 0 2) peak intensity increased as the rGO ratio increased from 0 wt% to 1 wt%; however, the intensity decreased with an increase in the rGO ratio beyond 1.5 wt%. The carbon doping effect on ZnO has been intensively investigated for potential applications over the past several years [24–28]. Carbon can occupy either Zn (C<sub>Zn</sub>) or O (C<sub>O</sub>) sites during the doping process, depending on the annealing conditions. In the current investigation, while the AZO:rGO films were annealed in an Ar + H<sub>2</sub> atmosphere, carbon atoms might have occupied Zn<sup>2+</sup> vacancies to form C<sub>Zn</sub> defects [26–28].

Table 2 shows the structural parameters of the AZO:rGO films shown in Fig. 4. The crystalline plane distance (*d*) was estimated using the Bragg formula:  $\lambda = 2d\sin\theta$ , where  $\lambda$  is the X-ray wavelength (0.154056 nm) and  $\theta$  is the diffraction angle of the (0 0 2) peak. The lattice constant, *c*, is equal to 2*d* for the (0 0 2) diffraction peak. The strain ( $\epsilon$ ) of the films in the direction of the *c*-axis is given by the equation  $\epsilon =$

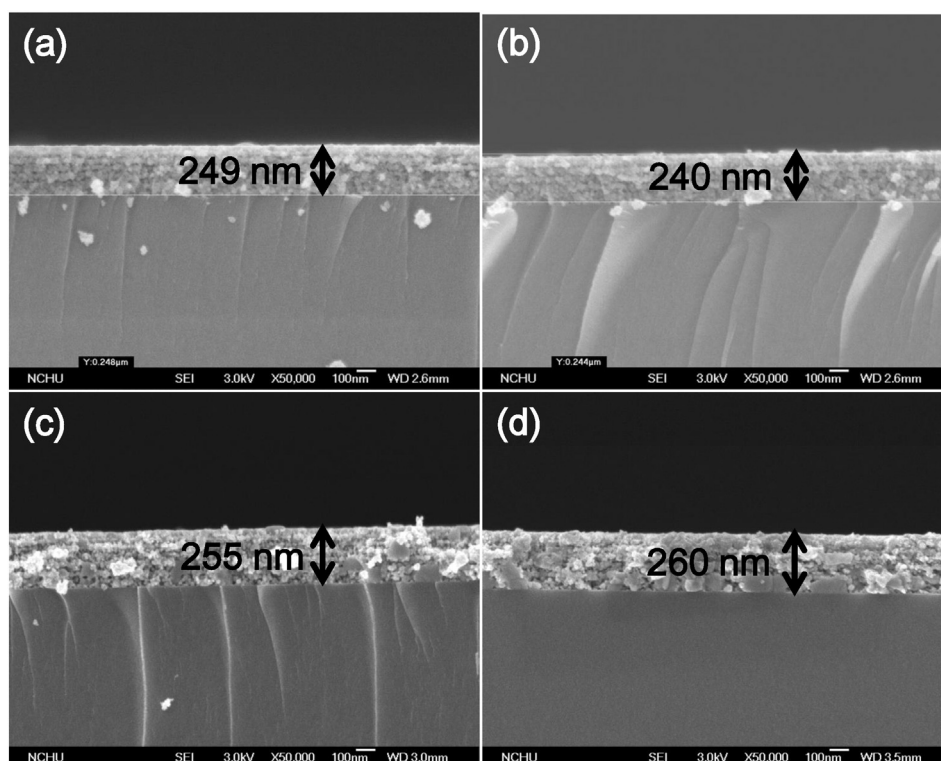


**Fig. 3.** Cross-section SEM images of the AZO:rGO thin films with different rGO ratios of (a) 0.0 wt%, (b) 1.0 wt%, (c) 1.5 wt%, and (d) 3.0 wt%.





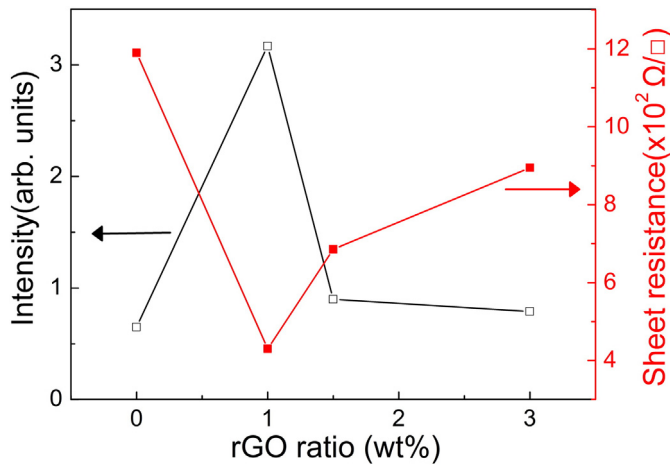


Fig. 6. Relationship between the sheet resistance and the XRD (0 0 2) peak intensity.

Fig. 9(a) and 9(b) shows the sheet resistance, carrier concentration, and Hall mobility of AZO:rGO thin films as a function of the rGO ratio. The rGO sheet resistance could be effectively reduced by increasing the rGO ratio to a high value. The sheet resistance of AZO:rGO thin films with 1 wt% rGO decreased by a factor greater than two compared with that in the absence of rGO; however, for rGO ratios above 1 wt%, the sheet resistance increased with the rGO ratio. The Hall mobility and carrier concentration increased from 9.1 to 15.1  $\text{cm}^2/\text{V}\cdot\text{s}$  and from  $2.41 \times 10^{19}$  to  $8.27 \times 10^{19} \text{ cm}^{-3}$ , respectively, for an increase in the rGO ratio from 0 to 1.0 wt%. The lowest sheet resistance was  $430 \Omega/\square$ . The carrier concentration and Hall mobility increased with the rGO concentration and reached the maximum for the rGO concentration of 1.0 wt%. The increase in the Hall mobility with the rGO ratio was due to the enhanced crystallinity of the films. A decrease in the carrier concentration for rGO ratios above 1.0 wt% may be ascribed to the reduced crystallinity of the films, as indicated by the XRD diffraction pattern in Fig. 4. The increase in the Hall mobility of AZO:rGO films was because of the combined effect of an increase in the grain size and a decrease in the sheet resistance, both of which enhanced the crystallinity [31].

The time-dependent resistivity of AZO:rGO thin films with different rGO ratios is shown in Fig. 10. The possibility of the film sheet resistance increasing with time may be due to the adsorption of oxygen: the film surface absorbs oxygen from the air, leading to a decrease in the free

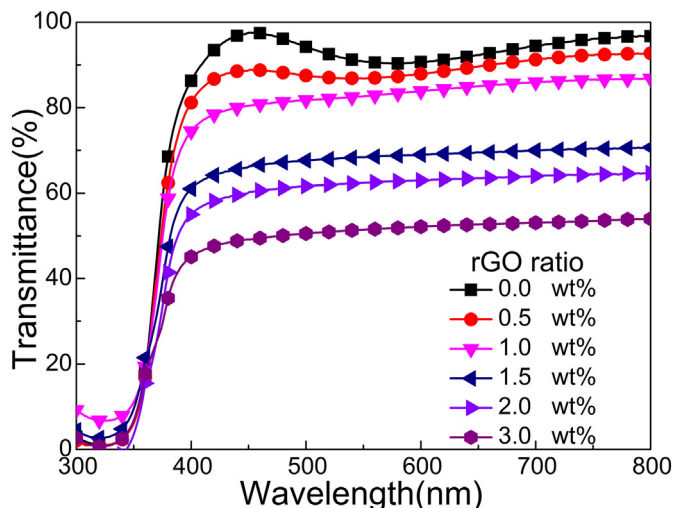


Fig. 7. Optical transmittance of the AZO:rGO thin films with different rGO ratios.

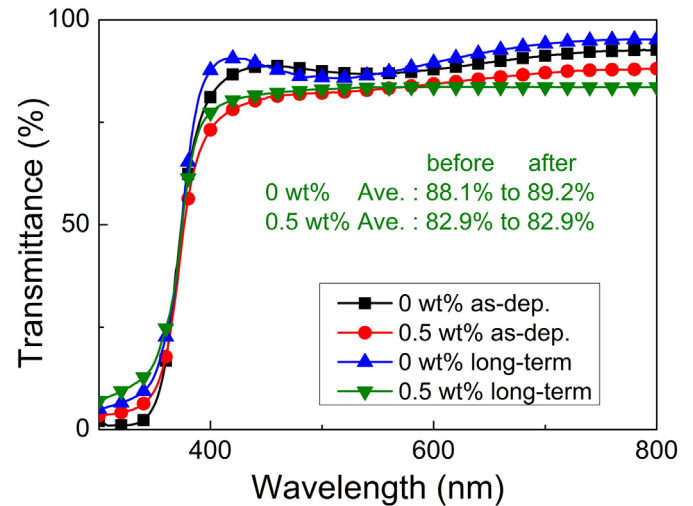


Fig. 8. Optical transmittance of the AZO:rGO thin films before and after long-term stability test.

electron and carrier concentrations [32]. However, after eight days, the sheet resistance did not change noticeably because oxygen adsorption became saturated.

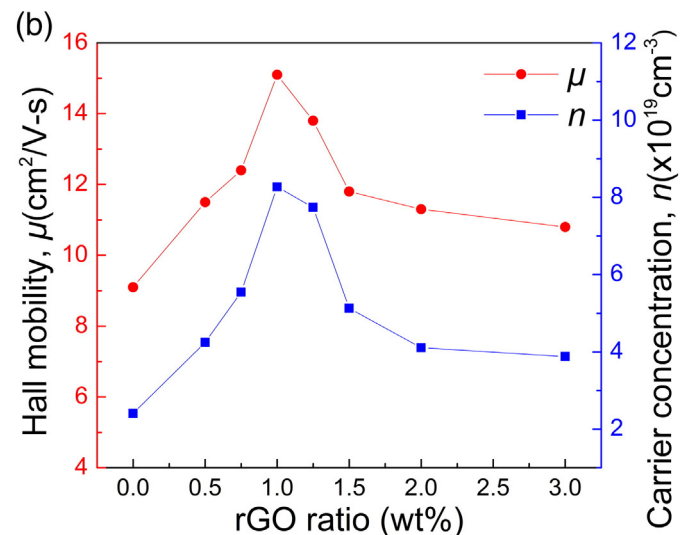
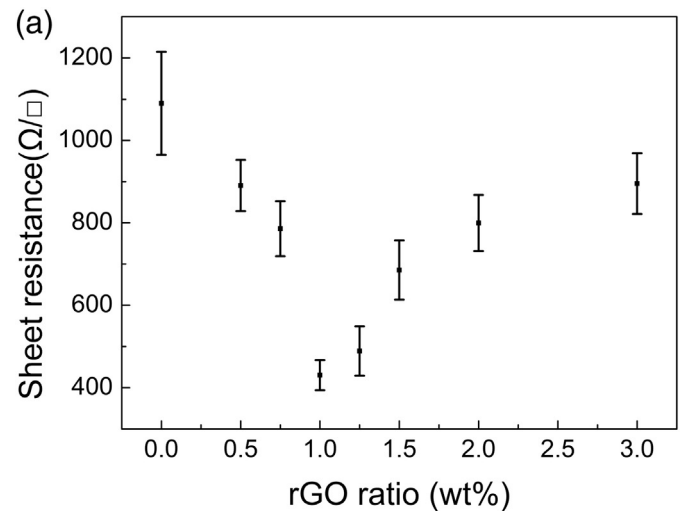


Fig. 9. (a) Sheet resistance and (b) Hall mobility and carrier concentration of the AZO:rGO thin films with different rGO ratios.

